Global and Planetary Change 100 (2013) 278–290

Contents lists available at SciVerse ScienceDirect

Global and Planetary Change

journal homepage: www.elsevier.com/locate/gloplacha

Combining ice core records and ice sheet models to explore the evolution of the East Antarctic Ice sheet during the Last Interglacial period

S.L. Bradley [a,*], M. Siddall [b], G.A. Milne [c], V. Masson-Delmotte [d], E. Wolff [a]

[a] British Antarctic Survey, Madingley Road, Cambridge, UK
[b] Department of Earth Sciences, University of Bristol, Bristol, UK
[c] Department of Earth Sciences, University of Ottawa, Ottawa, Canada
[d] Laboratoire des Sciences du Climat et de l'Environnement (IPSL/CEA-CNRS-UVSQ UMR 8212), Gif-sur-Yvette, France

ARTICLE INFO

Article history:
Received 24 August 2012
Accepted 5 November 2012
Available online 12 November 2012

Keywords:
Isostasy
Ice cores
Antarctic Ice Sheet
Eustatic sea level
Last Interglacial
Ice sheet models

ABSTRACT

This study evaluates the influence of plausible changes in East Antarctic Ice sheet (EAIS) thickness and the subsequent glacio-isostatic response as a contributor to the Antarctic warming indicated by ice core records during the Last Interglacial period (LIG). These higher temperatures have been estimated primarily using the difference in the δD peak (on average ~15‰) in these LIG records relative to records for the Present Interglacial (PIG). Using a preliminary exploratory modelling study, it is shown that introducing a relatively moderate reduction in the amount of thickening of the EAIS over the LIG period introduces a significant increase (up to 8‰) in the predicted elevation-driven only δD signal at the central Antarctic Ice sheet (AIS) ice core sites compared to the PIG. A sensitivity test in response to a large prescribed retreat of marine-based ice in the Wilkes and Aurora subglacial basins (equivalent to ~7 m of global mean sea-level rise) results in a distinct elevation signal that is resolvable within the ice core stable isotope records at three sites (Taylor Dome, TALDICE and EPICA Dome C). These findings have two main implications. First, EAIS elevation's only effects could account for a significant fraction of the LIG warming interpreted from ice core records. This result highlights the need for an improved estimate to be made of the uncertainty and size of this elevation-driven δD signal which contributes to this LIG warming and that these effects need to be deconvolved prior to attempting to extract a climatic-only signal from the stable isotope data. Second, a fingerprint of significant retreat of ice in the Wilkes and Aurora basins should be detectable from ice core δD records proximal to these basins and therefore used to constrain their contribution to elevated LIG sea levels, after accounting for ice sheet–climate interactions not considered in our approach.

1. Introduction

Global mean sea level (GMSL) during the Last Interglacial (LIG) is estimated to have been between 5.5 and 10 m higher than that during the present interglacial (PIG) (Kopp et al., 2009; Dutton and Lambeck, 2012). A number of recent studies have considered the possible contributions to this higher sea level. For example, thermal expansion of the ocean produced ~0.4 ± 0.3 m of GMSL rise (McKay et al., 2011) and melting from valley glaciers and small ice caps could have contributed up to ~0.6 ± 0.1 m (Radi and Hock, 2010). It is generally agreed that by far the largest contribution must have come from the major ice sheets; 0.4–4.4 m from the Greenland Ice sheet (Cuffey and Marshall, 2000; Otto-Bliesner et al., 2006; Robinson et al., 2011; Helsen et al., 2012; Quiquet et al., 2012; Stone et al., 2012; Helsen et al., submitted for publication) and 3–6 m from the Antarctic Ice Sheet (Bamber et al., 2009; Kopp et al., 2009; Gomez et al., 2010; Bradley et al., 2012). Recent findings from the NEEM ice core (NEEM community members, in revision) and from ice sheet simulations (Robinson et al., 2011; Helsen et al., 2012, Quiquet et al., 2012; Stone et al., 2012; Born and Nisancioglu, 2012; Helsen et al., submitted for publication) suggest a limited (~2 m) contribution of the Greenland ice sheet, thereby increasing the magnitude of the contribution required from Antarctica.

Until recently, the central East Antarctic Ice sheet (EAIS) was considered to have been relatively stable throughout the Pleistocene glacial–interglacial cycles, with changes in ice sheet surface elevation estimated to have been ~100 m (Haywood et al., 2002; Lilly et al., 2010; Liu et al., 2010). However, recent studies concluded that large areas of the EAIS may be susceptible to rapid mass loss (or retreat) and that the size of the ice sheet may therefore have been reduced during the LIG compared to the PIG (Jordan et al., 2010; Pierce et al., 2011; Pingree et al., 2011). This implies that the question of EAIS stability needs to be readdressed for the LIG. This study aims to explore this using a comparison between ice core observations and simulations of ice surface elevation changes (including that due to the isostatic response of the solid Earth, a process more commonly referred to as glacial isostatic adjustment (GIA)).

* Corresponding author. Tel.: +44 7889469890.
E-mail address: d80ngv@gmail.com (S.L. Bradley).

0921-8181/$ – see front matter © 2012 Elsevier B.V. All rights reserved.
http://dx.doi.org/10.1016/j.gloplacha.2012.11.002

One proposed region of large and potentially rapid mass loss is within the Wilkes and Aurora subglacial basins (abbreviated within this study to W–A basins, see Fig. 1). Across this region, where the ice is grounded below sea level, the overlying ice sheet is more vulnerable to the impact of changes in ocean temperature. Only one study to date has explored the possible contribution to GMSL from the retreat of ice in this region. Gomez et al. (2010) estimated that if all marine-grounded ice was to melt within the W–A basins (see their Fig. 1) GMSL would increase by ~18 m. This is an extreme scenario and it is used here to highlight that this sector of the EAIS has the potential to add a significant contribution to GMSL (relative to the PIG).

There are a number of recent studies which have proposed that the surface temperature of the EAIS was significantly warmer during the four preceding interglacial cycles (MIS5, MIS7, MIS9 and MIS11) compared to the PIG (see Holden et al., 2010; Masson-Delmotte et al., 2010; Lang and Wolff, 2011). This finding is estimated primarily using the 800 kyr EPICA Dome C stable water isotope ice core record (δD) (see Fig. 2a Lang and Wolff, 2011) by comparing the magnitude of the Antarctic interglacial peak during each of these cycles to that during the PIG. For the LIG (or during MIS5), the six available EAIS ice core water stable isotope records (see Figs. 1 and 2) show an early interglacial δD peak above PIG levels at an average 15‰ (Holden et al., 2010; Masson-Delmotte et al., 2011). This feature is commonly referred to as the 'LIG overshoot'.

Isotope-temperature relationship studies have interpreted the LIG overshoot to suggest temperature anomalies at least 2–5 °C above present-day values (Jouzel et al., 2007; Sime et al., 2009; Masson-Delmotte et al., 2011; Uemura et al., 2012). However, a range of factors contribute to and drive the observed signal in these ice core observations and so a robust interpretation is not straightforward. These include changes in temperature, moisture origin (Stenni et al., 2010; Uemura et al., 2012) and precipitation intermittency (Laepple et al., 2011) and site elevation (resulting from both changes in ice thickness and movement of the solid land surface) (see Masson-Delmotte et al., 2011). While climate models do not produce significant Antarctic warming in response to LIG orbital forcing (Holden et al., 2010; Masson-Delmotte et al., 2010), when changes in West Antarctic ice sheet (WAIS) topography were combined with a bipolar seesaw linked with ocean circulation in such a models, an EAIS warming was produced comparable to the signal derived from ice cores (Holden et al., 2010).

Past research into interpreting the factors driving these higher δD peaks has attributed most of the signal to changes in Antarctic

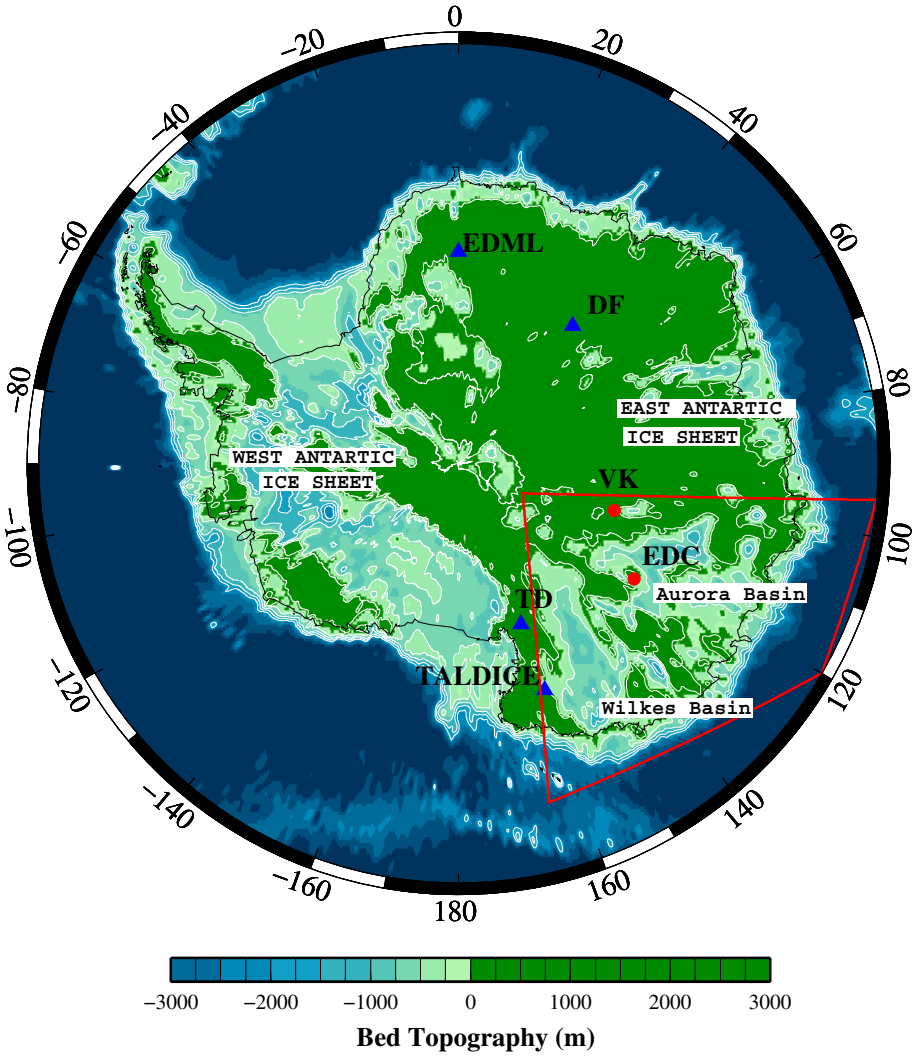

Fig. 1. Contoured bedrock topography (m) using the data set from Le Brocq et al., 2010. The location of the six ice core sites (summarised in Table 1) are shown, with associated abbreviated names and symbols. Also highlighted by the solid red box is the approximate location of the Wilkes and Aurora subglacial basins.

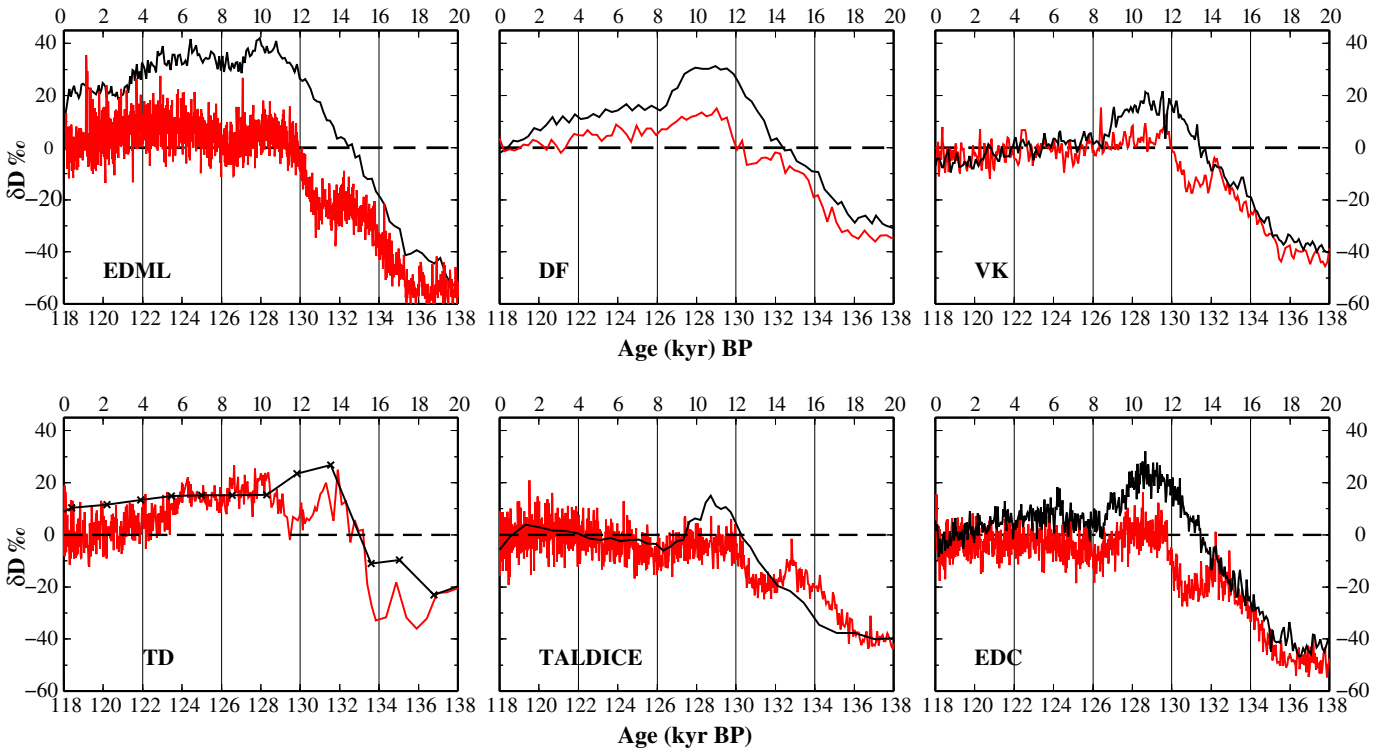

Fig. 2. Comparison of the stable water isotope records, converted to δD, at the six ice core sites for a time interval spanning the PIG (0–20 kyr BP; red line) and the LIG (118–139 kyr BP; black line). Note that crosses are shown on the Taylor Dome (TD) record to emphasise the lower resolution of this record.

climate. However, a possible factor contributing to this LIG overshoot during MIS5, and also the earlier higher interglacial peaks (MIS7,9 and MIS 11) in the ice core observations are the influence of changes in surface elevation driven by changes in ice thickness and movement of the solid land surface (SLS) (through the process of GIA).

This study follows the method adopted in Bradley et al. (2012) and Siddall et al. (2012) to consider the impact of changes in surface elevation on the interpretation of LIG ice core records based on a comparison between GIA modelling and ice core evidence. A GIA model is a geophysical model which can be used to compute the height of the SLS in Antarctica due to a time-varying ice-ocean load.

This paper is the first to investigate EAIS evolution during the LIG using such a method. It takes advantage of spatial and temporal information available from six Antarctic ice core records (Section 2) combined with GIA modelling (Section 3). Three different, but plausible ice sheet scenarios were established (Section 3) to focus on the two issues outlined above: (1) whether an elevation driven response may represent an important contribution to the inference of higher LIG temperatures and (2) whether the ice core records are sensitive to a possible collapse of marine-based ice in the W–A basins.

2. Ice core data

There is sparse direct evidence (i.e. geomorphological field observations such as periglacial trimlines or moraines) to constrain ice model reconstructions for the LIG (Bradley et al., 2012). Thus there is a need to rely upon indirect evidence such as far-field sea level data (Kopp et al., 2009) or paleoclimate data (McKay et al., 2011)) which are more complicated to interpret because of their dependence on other ice sheets and/or processes within the climate system (see Masson-Delmotte et al., 2011; Bradley et al., 2012). Stable water isotope records obtained from ice cores (e.g. $\delta^{18}O$ or δD) are a subset of paleoclimate data and, at present there are records available from six sites located across the EAIS (Fig. 1 and Table 1).

2.1. Ice core data: corrections and age models

Numerous factors drive changes in the ice core stable water isotope record (see Masson-Delmotte et al., 2011 for a full discussion). This study will focus primarily on the influence of variations in surface elevation in driving the observed signal. We note that variations in surface temperature will also be an important factor contributing

Table 1
Summary details of the six ice core data sets and associated references used within this paper, with core locations shown on Fig. 1. Sites where the original data was accessed as δD or $\delta^{18}O$ are displayed on Fig. 1 as a red circle or blue triangle respectively. These different symbols are used throughout the paper.

Site	Name	Symbol	Longitude	Latitude	Data	No. of points	Source
Taylor Dome	TD	▲	158.717	−77.8	$\partial^{18}O$	13	Grootes et al., 2001
Talos Dome	TALDICE	▲	159.1	−72.8	$\partial^{18}O$	39	Stenni et al., 2010
Vostok	VK	●	106.8	−78.47	∂D	309	Jouzel et al., 1993
EPICA Dome C	EDC	●	123.38	−75.1	∂D	424	Jouzel et al., 2007
Dome Fuji	DF	▲	39.7	−77.317	$\partial^{18}O$	64	Watanabe et al., 2003
EPICA Dronning Maud Land.	EDML	▲	0.067	−75	$\partial^{18}O$	176	EPICA members, 2006

to the observed ice core signals but these have been considered previously and so we focus on the former process. For example, an increase in the observed δD ice core signal may be generated by both/either an increase in temperature and/or a fall in surface elevation. This study will explore the elevation-driven δD signal associated with changes in the evolution of the EAIS and the accompanying solid earth response over the LIG (138–118 kyr BP).

First, ice core records for the two most recent periods that include a termination and an interglacial – Termination 2 plus the LIG (138–118 kyr BP) and Termination 1 plus the PIG (20–0 kyr) – will be compared (Fig. 2). These 20 kyr intervals were adopted to represent the transition from glacial-interglacial conditions, between the Penultimate Glacial Maximum (PGM) and Last Glacial Maximum (LGM) (~140 and 21 kyr BP, respectively) to the later part of each interglacial period in Antarctica (118/0 kyr BP, respectively).

There are six available EAIS ice core stable water records, either as $\delta^{18}O$ or δD, which extend over the time intervals defined above. In order to create a consistent framework for comparison, all the $\delta^{18}O$ records were converted in terms of unit of δD equivalence, using the global meteoric water line slope of 8 (Masson-Delmotte et al., 2008) and each record was referenced to a late-Holocene average (mean over the last 3 kyr) defined from the initial data records. These records extend from the start of the PGM to the present day. The EDC3 age scale (Parrenin et al., 2007) was adopted for all six ice core records. The locations, references and acronyms are summarised in Table 1 with a more detailed description of the data inter-site variability and the range of factors driving the observed trends given in Masson-Delmotte et al. (2011). All six sites are located across the East Antarctic Plateau, with three sites (VK, DF and EDC) above 3000 m and three sites (TALDICE, TD and EDML) below 3000 m elevation and closer to the coast. Although the database is limited to only six records, it provides a reasonably even geographic spread across the EAIS, with EDML and DF located in a region of the ice sheet facing the Atlantic ocean; VK and EDC facing the Indian ocean and TD and TALDICE on the southern edge of the East Antarctic Plateau, facing the Ross Sea. Amongst these sites, EDML and VK are not located on dome summits and their isotopic variations are affected by changes in the upstream initial origin of the ice (Masson-Delmotte et al., 2011).

In order to compare the predictions of surface elevation generated from the GIA model and associated ice models with the ice core records, these results need to be converted into an equivalent change in δD. This requires an estimate of the relationship between changes in elevation and δD, which is known to be complicated, varying both spatially and temporally across an ice sheet due to changes in climate conditions (such as variations in the moisture and changes in temperature) (see Vinther et al., 2009; Masson-Delmotte et al., 2011). A recent study that examined Antarctic modern surface data calculated an average value lapse rate of $-0.074‰\ m^{-1}$ ($0.116\ °C\ m^{-1}$) decreasing to $-0.06‰\ m^{-1}$for data from only the WAIS and increasing to $-0.08‰\ m^{-1}$ ($0.113\ °C\ m^{-1}$) for all sites above 2000 m (e.g. Masson-Delmotte et al., 2008). As all the ice core sites are located at average present day elevations of >2000 m, an average value of $-0.08‰\ m^{-1}$ will be adopted for this study. It is noted that this value may have been both spatially and temporally variable during the LIG but currently there has been no study to fully explore this variability.

2.2. Data interpretation: comparing the PIG and LIG records.

On comparing the observed δD records (Fig. 2), there are some key similarities and differences, which are summarised below.

It is apparent that the magnitude of the minimum at the onset of the interglacial (138/20 kyr BP) and rate of rise from this minimum is similar for the two periods considered at each individual site (compare the black and red lines at each ice core site). In contrast, the size of the maximum δD peak (~128/10 kyr BP) which is taken to indicate the timing of the climate optimum/peak temperature across AIS (see Holden et al., 2010) is higher during the LIG compared to the PIG, on average ~15‰. For example at DF the maximum δD peak is 15‰ and 31‰ for the PIG and LIG respectively. Following this peak, over the next 2 kyr interval, most sites show a sharp fall in the δD (more pronounced over the LIG) with a secondary plateau above PIG values for some sites (EDML, EDC, DF). Following this, there is a gradual decline towards the later part of each interglacial to values close to present day values. There are some differences in the pattern towards the end of the LIG (between 126 and 118 kyr BP), which will be discussed further below.

Over these two time intervals, the δD glacial levels (at the PGM/LGM) and their rates of changes (a rise on average of 60‰) following the start of these terminations (prior to the Antarctic Cold Reversal for Termination 1) are relatively consistent. This can be taken to infer a broadly similar climate and/or elevation signal driving the observed trend at each of the ice core sites. It is noted that there will differences in the style of retreat between these two glacial cycles towards the later part of the interglacial (as illustrated on Fig. 2), specifically after the Antarctic Cold Reversal during Termination 1 for example.

The LIG overshoot feature (Sime et al., 2009; Stenni et al., 2010; Uemura et al., 2012) is clearly identifiable on Fig. 2, with the higher peak in the δD (up to 15‰) at ~128 kyr BP during the LIG compared to the PIG at ~10 kyr BP). One of the main aims of this paper is to explore the contribution of changes in ice surface elevation to this δD signal. For example, a reduction in ice surface elevation during the LIG relative to the PIG would produce a positive δD signal that is equivalent to the effect of warming local air mass.

While the EAIS stable isotope records are similar over the early LIG interval, towards the end of this period (126–118 kyr BP) there is greater inter site variability. The possible driving mechanisms of this variability are described in greater detail in Masson-Delmotte et al. (2011) and Bradley et al. (2012). This study does not explore in any detail these smaller, short time scale differences. However, there are two main differences which are worth highlighting that may imply differences in the behaviour of the EAIS between sites towards the end of the LIG. At TALDICE there is a small rise in δD (~0‰) sustained for 6 kyr, compared to a steady fall at the other five sites, ranging from −20‰ (DF) to <5‰ (VK). This spatial variability may be recording differences in either the local climate at these sites (Sime et al., 2009) or a pattern of ice sheet growth/retreat and accompanying impact on ice surface elevation. For example, Bradley et al., 2012 found that it was possible to reproduce this rise in the δD at TALDICE by introducing an increased thinning in the EAIS along the eastern edge of the Ross Sea which led to a fall in surface elevation, a factor which was discussed in Masson-Delmotte et al., 2011.

3. Method

3.1. GIA model

At each ice core site, predictions of changes in surface elevation will be generated due to (a) changes in ice thickness only calculated from the range of input ice models described in Section 3.2, (b) vertical movement of the SLS only, (c) final total surface elevation change (i.e. the combination of (a) and (b)).

To generate the predictions of changes in surface elevation due to the vertical movement of the SLS, a GIA model is used. A GIA model calculates the isostatic response of the solid Earth due to a defined surface mass redistribution between grounded ice and the ocean. The model has three key components: a model of grounded ice evolution (see Section 3.2); an Earth model to reproduce the solid Earth deformation resulting from the surface mass redistribution (between the ice sheets and oceans) and a model of sea-level change to calculate the redistribution of ocean mass (e.g. Farrell and Clark, 1976).

The first two are model inputs defined by the user and will be varied within this study.

The input Earth model is a spherically symmetric, self-gravitating Maxwell body, in which the elastic and density structure are taken from a seismic model (Dziewonski and Anderson, 1981), with a depth resolution of 10 km within the crust and 25 km in the mantle. The viscous structure is more crudely parameterized into three layers: a high viscosity (10^{43} Pa s) outer shell to simulate an elastic lithosphere, an upper mantle region of uniform viscosity extending from beneath the lithosphere to the 660 km seismic discontinuity and a lower mantle region of uniform viscosity extending from this depth to the core–mantle boundary. The lithosphere thickness and viscosity values within the upper and lower mantle are user defined parameters in the modelling. The viscosity structure beneath the Antarctic continent is most likely characterised by significant lateral variability (Morelli and Danesi, 2004). Three Earth models are considered which aim to encompass some of this variation: an intermediate model with a lithosphere thickness of 96 km, upper and lower mantle viscosities of 5×0^{20} Pa s and 1×10^{22} Pa s, respectively; a model to represent the region below the West Antarctic Archipelago, which is characterised by a relatively high heat flow and so a thinner lithosphere (71 km) and weaker upper mantle (1×10^{20} Pa s); and, finally, a model more typical for colder continental cratons such as that below the EAIS, with a thicker lithosphere (120 km) and greater upper mantle viscosity (1×10^{21} Pa s). Note that the viscosity of the lower mantle is the same in each of the models considered. The parameters considered are broadly compatible with values inferred in previous GIA studies (e.g. Forte and Mitrovica, 1996; Davis et al., 1999; Kaufmann and Lambeck, 2002).

Within the GIA model, the redistribution of mass over the ocean basins (or relative sea-level change) is computed in a gravitationally self-consistent manner by solving the sea-level equation (Mitrovica and Milne, 2003; Kendall et al., 2005) that includes a number of relatively recent advances in GIA sea-level modelling: time-varying shoreline migration, an accurate treatment of the sea level change in regions of ablating marine-based ice and the influence of GIA perturbations in the Earth's rotation vector (Milne and Mitrovica, 1998; Mitrovica et al., 2001, 2005). Once the ice-ocean mass redistribution has been calculated, we compute vertical motion of the SLS using the spectral approach described in Mitrovica et al., 1994.

Given that the observed δD value is defined relative to an 'average present day value' (see Section 2), it is important to ensure the same reference point is used when predicting the final surface elevation at each ice core site, prior to converting into an equivalent δD. To address this, all final predictions were defined with respect to present day ice surface elevation. This is important for two key reasons: first to ensure a consistent reference point in time when comparing observed and predicted δD, and second to incorporate the effect of previous glaciations on the elevation changes over the LIG, when the system may not have returned fully to a state of equilibrium (as discussed in Lambeck et al., 2012).

3.2. Ice models

Three Antarctic ice models are used to calculate changes in ice thickness at each ice core site. These models, described below, are (a) an Antarctic deglaciation model (Section 3.2.1) taken from Bradley et al., 2012 which will be used as a reference, and two models that are derived from this: (b) a model which includes a reduced amount of thickening of the EAIS during the early LIG period (see Fig. 3) (see Section 3.2.2.1), (c) a model which simulates a continued thinning and retreat within the Wilkes and Aurora basins (W–A basins) (see Fig. 4b) (see Section 3.2.2.2).

3.2.1. Reference ice model

The reference ice model (hereafter referred to as REF_L) is described in an earlier study (Bradley et al., 2012) and combines the results from three publications (a) one which developed a global ice sheet model (Bassett et al., 2005) and (b) two AIS models for the evolution of the ice sheet over the two most recent glacial-interglacial cycles: (i) for the PIG (as defined here between 21–0 kyr) (Bassett et al., 2007) and (ii) the LIG (Bradley et al., 2012) (230–118 kyr BP). Since this model (REF_L) is described in Bradley et al., 2012, the key elements only are summarised below.

The PIG AIS model (Bassett et al., 2007) was adapted from a glaciological model of the AIS (Huybrechts, 2002) and calibrated, for the evolution of the ice sheet during the PIG (Termination 1 to the Holocene), to a suite of near field and far-field relative sea level data. The present day extent of the AIS within this model will be used when referencing the predicted change in surface elevation over the LIG and subsequent conversion to δD.

For the LIG AIS model (Bradley et al., 2012), the chronology and pattern of deglaciation were constrained using the LIG ice core data (Fig. 2) as well as global far-field sea level records. The spatial extent at 135 kyr BP and predicted equivalent sea level (ESL) curve (defined relative to the Holocene) are illustrated on Figs. 3a and 4, respectively, with the total ESL contribution from the model during LIG (140–118 kyr BP) being ~18.7 m (−0.4 m and 19.2 m from the EAIS and WAIS respectively, see Table 2). Table 2 summarises the contribution to ESL from each ice model considered in this study.

It is noted that in all the AIS models developed within this paper the extent of the AIS during the PIG remains unchanged. For evolution of the AIS over the LIG, only the EAIS extent of the REF_L model is altered with the extent of the WAIS unchanged. It is noted that within the REF_L model, the WAIS still undergoes a significant retreat as discussed in Bradley et al., 2012. It is important to note, however, that the WAIS retreat in this model does not result in an elevation signal at EAIS core sites (Bradley et al., 2012).

Following the PGM, the ice sheet undergoes two main phases of mass change: (i) between 135 and 126 kyr BP, there is a significant retreat and thinning across all areas of the WAIS, which drives a ~20 m rise in ESL, but a minor thickening (due to an increase in accumulation rates) of the EAIS (~150 m at each ice core site) to produce a fall in ESL of ~1 m; (ii) between 126 and 118 kyr BP, there is a smaller but continued retreat across the WAIS and a minor thinning (~50 m) across some regions of the EAIS, which together drive a total rise in ESL (~3 m see Fig. 4).

3.2.2. Development of two new models for the evolution of the EAIS over the LIG.

In this section, two new models for the evolution of the AIS over the LIG are generated by adapting the REF_L model: (a) a model with a reduced amount of thickening of the EAIS during the LIG, which will be referred to as REF_THIN (Section 3.2.2.1), (b) a model which recreates an idealised retreat within the W-A basins. This model will be referred to as REF_WB (Section 3.2.2.2). In both of these models only the EAIS component of the REF_L model will be altered, with the WAIS component and all other ice sheets remaining unchanged.

As briefly mentioned in the Introduction, few studies have focused on the evolution and mass changes of the EAIS during the LIG. This is due partly to the distinct lack of direct quantitative evidence of ice extent/evolution as most regions of the EAIS are still ice covered and any LIG signatures will have been overprinted by subsequent changes. Historically, literature on the EAIS evolution throughout the Pleistocene suggests that the EAIS was relatively stable, with changes in surface elevation estimated to be on the order of ~100 m (see Haywood et al., 2002; Huang et al., 2008; Lilly et al., 2010; Liu et al., 2010). Although most of the research concentrated on the evolution of the ice sheet over the PIG or earlier glacial cycles during the Pleistocene rather than the LIG, this was the viewpoint on which the majority of LIG EAIS ice sheets models were developed. However, it is notable that these earlier studies did highlight some controversy regarding the assumption of

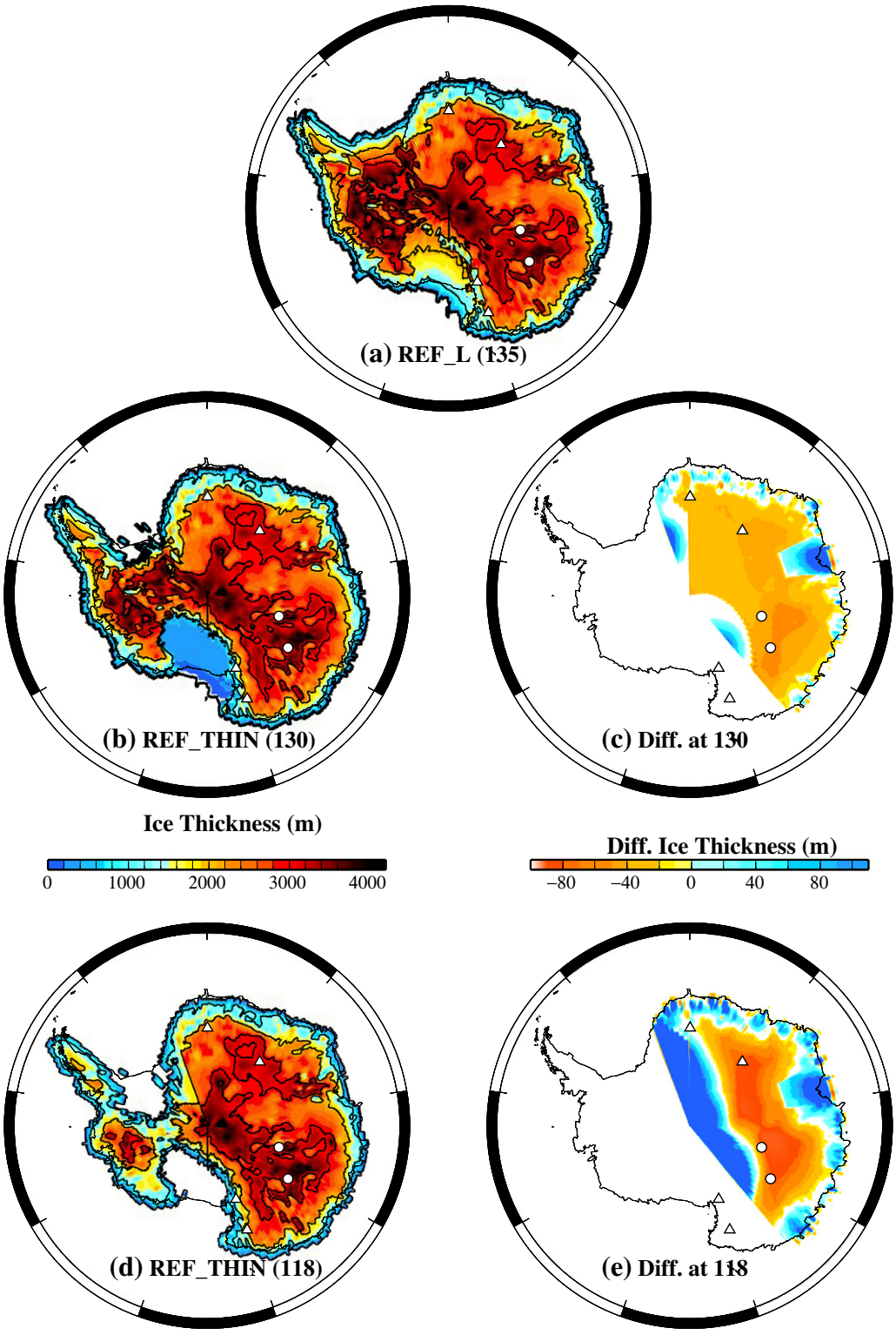

Fig. 3. The ice thickness at various time slices for the following ice models: (a) REF-L at 135 kyr BP; (b) REF_THIN at 130 kyr BP and (d) REF_THIN at 118 kyr BP. Plots (c) and (e) illustrate the difference in the ice thickness between the REF_L and REF_THIN ice model at 130 and 118 kyr BP, respectively. The sharp boundary evident in these plots results from the division of the Antarctic ice sheet into two regions to represent the West and East Antarctic ice sheets separately. In these plots, negative/positive values show regions in which REF_THIN is thinner/thicker compared to REF_L. The white regions on plots (c) and (e) mark regions of where there is no change in the ice extent. Also marked is the location of the six ice core sites as marked on Fig. 1 with additional information given in Table 1.

EAIS stability during the LIG which is now further supported by more recent studies (Hill et al., 2007; Jordan et al., 2010; Huybrechts et al., 2011; Pingree et al., 2011; Wright et al., 2012) which explore the behaviour of the EAIS during warmer climatic periods (such as the Pliocene). These latter studies infer that during a glacial-interglacial period in which the interglacial temperature is warmer than the average for the late Holocene, the EAIS may be less stable. Under such conditions, the ice sheet may retreat to a smaller final extent compared to that seen for the PIG, either due to a reduced amount of thickening or an increased mass loss due to significant retreat in a subglacial basin.

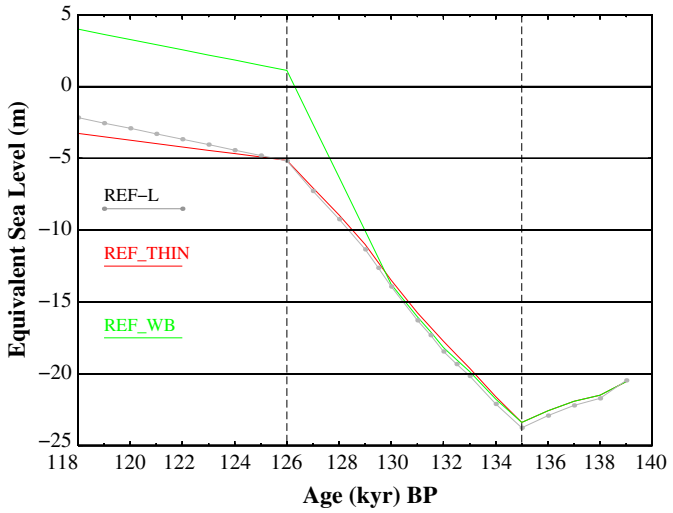

Fig. 4. The predicted equivalent sea level change due to the Antarctic Ice Sheet relative to the present day for the REF_L model (grey line), REF_THIN model (red line) and REF_WB model (green line). The two dashed black vertical lines mark the timing of the onset of deglaciation of the AIS (135 kyr BP) within the revised ice sheet models and the approx. timing of the global highstand (126 kyr BP).

Therefore, to recreate the behaviour of the EAIS over the LIG, studies on the response of the EAIS during the Pliocene were used as a guide. It is noted that the purpose of these models is to perform an initial sensitivity study to examine plausible variations in elevation-driven δD. Thus, the ice models are based on end member scenarios and they capture, somewhat crudely, the key features of these scenarios. Furthermore, we do not account for the climate impacts of changes in ice sheet topography and meltwater fluxes.

3.2.2.1. Development of the REF_THIN ice model. The aim of the REF_THIN model is to explore the impact of reduced EAIS thickening over the LIG (compared to the PIG) on the elevation-driven δD signal. To produce the REF_THIN model, a similar method to that used in the development of the REF_L model (as described in Bradley et al., 2012) was adopted: the timings of changes in the observed δD records (see Fig. 2) are used to constrain the timings of the thickening/thinning of the EAIS during the LIG.

Between 135 and 130 kyr BP (to coincide with the early rise in the δD record, see Fig. 2), the amount of relative thickening across the EAIS within the REF_L is reduced by half. From 130–118 kyr BP, the peripheral thinning in the REF_L model (across Queen Maud Land) (Bradley et al., 2012) has been removed so that the extent of EAIS is fixed over this period. This later revision to the REF_L model is more consistent with the pattern of surface elevation change across the EAIS simulated in other AIS ice sheet models (Lilly et al., 2010; Denton, 2011; Mackintosh et al., 2011; Whitehouse et al., 2012).

The spatial extent of the REF_THIN model at 130 and 118 kyr BP and differences of this model relative to REF_L are shown on Fig. 3(c and e). The ESL curve for REF_THIN is shown on Fig. 4 and summarised in Table 2. In Fig. 3(c and e), a negative change in ice thickness indicates regions of REF_THIN which are thinner compared to REF_L (e.g. the central EAIS regions of Fig. 3c). A positive difference in ice thickness is where the REF_THIN model is now thicker than the REF_L model, such as shown along the outer edges of Fig. 3e, which is where the thinning in REF_L (across Queen Maud Land) towards the later part of the LIG is removed. The total contribution to ESL is reduced using the REF_THIN model by ~1 m from the REF_L model, to ~17.7 m (between 140 and 118 kyr BP), with (−) 1.22 m from the EAIS only (compared to (−) 0.4 m in REF_L model).

At each ice core site the reduction in the predicted increase in the surface elevation due to changes in ice thickness varies temporally within the REF_THIN model; for example at most sites the difference (relative to REF_L model) at 130 kyr BP is ~−40 m, compared to ~−80 m by 118 kyr BP. At all sites and over the LIG interval, the total amount of thickening is reduced from 150 m in the REF_L model to 80 m in REF_THIN, which is compatible with estimates from other studies at these sites using other AIS models (as discussed above).

Because the total model contribution of the EAIS to ESL is minor in comparison to the WAIS, the impact of these revisions in the REF_THIN on the total ESL change (see Fig. 4) is more evident when examining the predicted ESL from this sector of the AIS only (see Table 2). This revised model (REF_THIN) now produces a fall in ESL ~1.2 m (compared to a fall 0.43 m in REF_L). This large difference between the two models is due to the removal of the later thinning (between 126 and 118 kyr BP) in the REF_L, which added +1.10 m rise to the total EAIS ESL contribution over this interval, thus offsetting most of the effect of the earlier reduced thickening.

3.2.2.2. Development of the REF_WB, Wilkes–Aurora basins retreat ice model. The concept of a significant retreat within one of the submarine basins within the East Antarctic Continent (see Fig. 1) is a new and relatively untested scenario (Jordan et al., 2010; Pierce et al., 2011; Pingree et al., 2011; Wright et al., 2012). To our knowledge, there are no published ice models which show such a feature. This is likely due to the limited amount of direct evidence to constrain or support such an event. However, newer and more recent studies (Pierce et al., 2011; Pingree et al., 2011; Wright et al., 2012) are now producing more direct evidence (such as offshore ice-rafted debris records, see Pierce et al., 2011) which indicate that such an event is likely to have occurred within the W-A basins during the LIG. Given this and the recent literature that indicates such an instability in the LIG EAIS is possible (see discussion above), we developed a model that includes an enhanced retreat of marine-based ice (compared to the PIG) within the W–A basins.

Such retreats of marine-based ice have only been investigated for the AIS within such regions of the WAIS (see Bradley et al., 2012 for a summary). Therefore, to develop a model which simulates a continued and significant (beyond that seen for the Holocene) retreat of the EAIS within the W–A basins, a similar approach was adopted as used for these WAIS models (e.g. Vaughan and Spouge, 2002; Bamber et al., 2009; Gomez et al., 2010; Bradley et al., 2012). These studies use the 'marine-based ice sheet instability hypothesis'

Table 2
Contributions to equivalent sea level (ESL) for the three Antarctic Ice sheet (AIS) models discussed in the text. The ESL is shown for the total interglacial period (140–118 kyr BP) and for three selected time intervals: 140–135 kyr BP, prior to the onset of deglaciation; 135–126 kyr BP, the main phase of deglaciation of the AIS, and 126–118 kyr, the final retreat phase from the AIS and the West Antarctic Ice sheet (WAIS) and East Antarctic Ice sheet (EAIS) separately.

	REF-L			REF_THIN			REF_WB		
	AIS	EAIS	WAIS	AIS	EAIS	WAIS	AIS	EAIS	WAIS
Total	18.72	−0.43	19.15	17.76	−1.22	18.98	25.21	6.62	18.58
140-135	−3.38	−0.42	−2.96	−2.92	−0.42	−2.50	−2.93	−0.44	−2.50
135-126	19.10	−0.97	20.07	18.78	−0.81	19.59	25.26	6.18	19.08
126-118	3.02	1.10	1.92	1.88	0.00	1.88	2.89	1.01	1.88

(Weertman, 1976; Mercer, 1978) where it is assumed that regions of the ice sheet which are marine based (i.e. grounded below present day sea level) and are located where there is a reverse sloping bed (i.e. ice margin retreats into deeper water) are more likely to destabilise and undergo continued collapse. Thus, we adopt the extent of marine grounded ice to define the spatial limits of EAIS retreat within the W–A basins in developing the REF_WB model.

It is noted that the term 'collapse' was used within the above studies to describe an enhanced and rapid retreat for marine-based regions of the WAIS. Given the distinctly different nature of the bed roughness/steepness which will affect the susceptibility of grounding line to undergo a significant retreat (see Siegert et al., 2005) of the two ice sheets, it is not implied that the retreat of the W–A basins would be as rapid as a WAIS sector collapse. For example, the marine regions of the EAIS within the W–A basins do not have such a strong reverse bed slope as for the majority of the WAIS. Therefore, in the REF_WB model, the EAIS undergoes an enhanced retreat beyond that for the PIG during a period of 4 kyr.

To define the spatial extent of the W–A basins, a recent dataset of the bedrock topography (Le Brocq et al., 2010; see Fig. 1) and the information given in some recent studies (i.e. Jordan et al., 2010; Young et al., 2011) were used as a guide. In addition, the spatial limits of any increased retreat within these basins is delimited laterally by the presence of LIG age ice at the TALDICE, TD and EDC ice core sites (see locations marked in Fig. 1). Combining these two constraints, the spatial extent of the continued retreat within the W–A basins is illustrated on Fig. 4b. The timing for this retreat was introduced between 130 and 126 kyr BP (a 4 kyr interval). This was to coincide with the approximate average timing of the global LIG highstand (~125/124 kyr BP) so that any contribution of the increased melt water to the GMSL occurs prior to the maximum in the sea-level observations.

The changes to the REF_L model in producing the REF_WB model are as follows: (1) prior to 130 kyr BP the AIS (including the EAIS and WAIS) remains unaltered from the REF_L model (see Fig. 5a); (2) Between 130 and 126 kyr BP, the EAIS now undergoes a continued mass loss with the W-A basins beyond that within the REF_L model, to the final extent shown in Fig. 5b; (3) between 126 and 118 kyr BP, the REF_WB follows the same retreat across the WAIS and other regions of the EAIS as within the REF_L model. We note that, the retreat of ice in REF_WB is similar, although less pronounced, to that considered in a recent study (Gomez et al., 2010). The predicted ESL of the REF_WB model is illustrated on Fig. 4 and summarised in Table 2, with an increased ESL rise (compared to REF_L) of 6.5 m to give a total AIS contribution of 25 m. The study of Gomez et al., 2010 gave an 18 m contribution from the Wilkes and Aurora basins since they simulated an entire retreat of both basins rather than only a component of each basin as done here (e.g. compare Fig. 4b to Gomez et al., 2010 Fig. 1).

4. Modelling results and discussion

Following the method outlined in Section 3, predictions of the isostatically-driven changes in surface elevation were generated at each ice core site for the REF_L, REF_THIN and REF_WB models. The predicted surface elevation change for each ice model was converted into an equivalent predicted elevation-driven δD (‰) signal (using the relationship described in Section 2.1) with the results shown for each of the three ice models (REF_L, REF_THIN and REF_WB) on Fig. 6.

Spatial plots of the predicted elevation-driven δD (‰/kyr) trend for the three ice models were generated over two time intervals (see Fig. 7): 135–130 kyr BP (Fig. 7a, b and c) and between 130 and 118 kyr BP (Fig. 7d, e and f). These results aim to show the impact, both spatially and temporally, of changing the evolution of the EAIS over the LIG and they complement the site-specific results shown in Fig. 6.

To complement the results shown on Fig. 6, results are shown on Fig. 8 for predicted surface elevation due to the movement of the SLS only for the three ice models. These results will highlight the impact of the on-going slower isostatic response in driving some of the inter-site variability in the response in the predicted δD signal towards the later part of the LIG when changes in the ice thickness were minimal.

In contrast to earlier studies (Bradley et al., 2012; Siddall et al., 2012) the impact of changing the viscosity structure was found to be significant in the new EAIS models. A deviation of up to 4‰ in the predicted elevation-driven δD using the different earth models was found which is greater than that obtained when investigating changes in the evolution of the WAIS (less than 1.4‰; Bradley et al., 2012). However, the relative impact of changing the ice model on

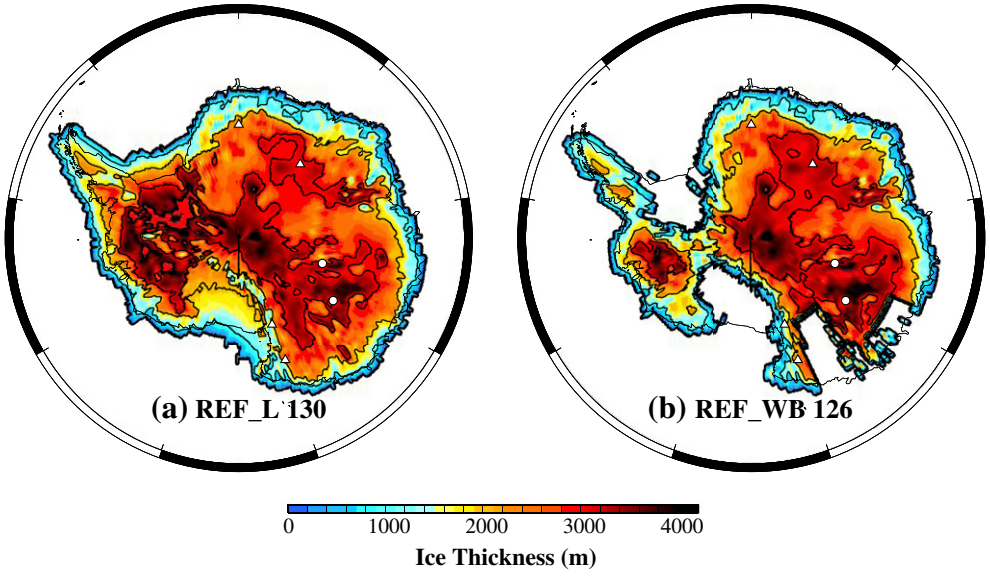

Fig. 5. Frames (a) and (b) show spatial plots of the ice thickness distribution for the REF_L at 130 kyr BP and REF_WB at 126 kyr BP respectively. Note that the continued retreat within the Wilkes and Aurora basins (see Fig. 1) in the REF_WB model is introduced between 130 and 126 kyr BP, with the ice model remaining unchanged from REF_L at all other times. Also marked is the location of the six ice core sites (Fig. 1) with additional information given in Table 1.

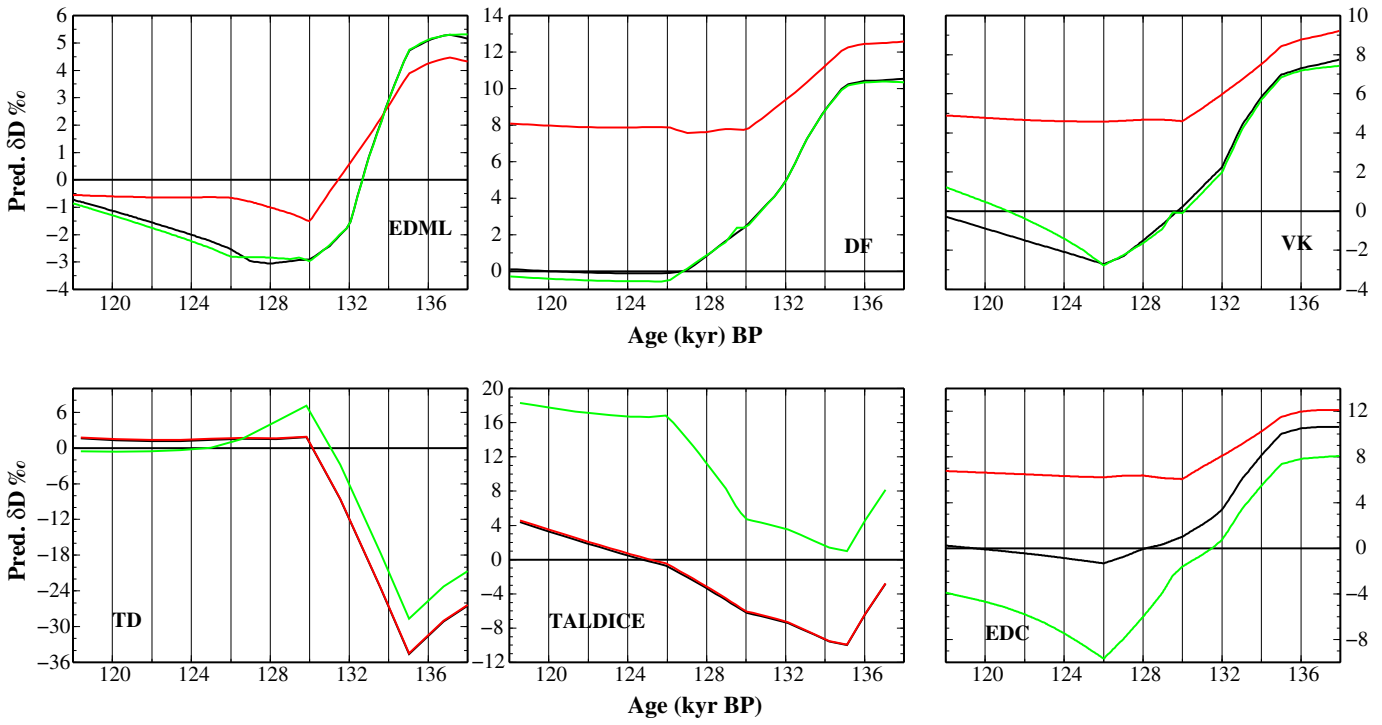

Fig. 6. The predicted elevation-driven δD (‰) signal at each ice core site for the three ice models described: REF-L (solid black line); REF_THIN (solid red line) and REF_WB (solid green line). Results are shown for the intermediate earth viscosity model only.

the predicted elevation-driven δD (‰) was, as before, found to be the larger and more significant factor in governing the surface elevation changes (compare results for REF_THIN to REF_WB in Fig. 6). Therefore the results in the following sections are described for the intermediate Earth model only (see Section 3).

4.1. Results for the REF_THIN ice model.

Examining the results illustrated on Fig. 6 (red line), Fig. 7b and e for REF_THIN model, several aspects of the differences in the spatial pattern and magnitude of the predicted elevation-driven δD (‰) signal are remarkable.

As found in a previous investigation (see Bradley et al., 2012) and shown on Figs. 6 and 7b, the spatial impact of the reduced amount of thickening of the EAIS (or a thinner EAIS) on the predicted elevation-driven δD (‰) signal is concentrated in regions which have experienced the greatest change in ice thickness (compare the spatial pattern of the δD results in Fig. 7b to spatial pattern of ice changes shown on Fig. 3c and e), which are predominately greatest across the central ice core sites (DF, EDC and VK). Changes in ice sheet thickness therefore dominate the central Antarctic predicted elevation-driven δD (‰) signal. However, over the later part of the LIG, when there is minimal change in the ice thickness, the on-going movement of the SLS (Fig. 8) to the preceding ice thickness changes becomes increasingly dominant and needs to be included in predictions.

Reducing the amount of thickening across the EAIS during the LIG within the REF_THIN model increased the magnitude of the predicted elevation-driven δD (‰) signal by up to 8‰ across these central sites (DF, VK, EDC) (see Fig. 6). Also the magnitude of the predicted elevation driven δD trend across this central EAIS region is increased by ~2‰/kyr between the REF_L and REF_THIN models (compare Fig. 7a and b). This is a significant change and is much larger than the response seen with plausible changes in the WAIS. (Bradley et al., 2012). The initial aim of the REF_THIN model was to investigate if altering the evolution of the EAIS could contribute significantly to the higher observed LIG δD peak or 'LIG overshoot' (on average 15‰, see Fig. 2). This result demonstrates that plausible changes in the evolution of the EAIS could contribute a significant signal at these central sites (DF, VK and EDC and EDML) and generate at least half of the observed δD (‰) peak at DF, EDC and VK. This is a factor that requires consideration when interpreting the various signals driving the observed δD changes. Ignoring the elevation effect when reconstructing LIG Antarctic air temperatures from ice core records could lead to significant error.

Inspection of Fig. 7b and e shows that the largest predicted elevation driven δD trend across the central EAIS ice core sites is generated during the first 5 kyr (see Fig. 7b, ~ − 3‰/kyr). This coincides with the largest magnitude response in both the ice thickness and movement of the SLS. Towards the end of interglacial (between 130 and 118 kyr BP, see Fig. 7e), the average predicted δD trend is significantly reduced at most of the sites (±0.2‰/kyr).

The removal of the thinning (hence relative rise in surface elevation) in the REF_THIN model compared to the REF_L model, during this final stage of the interglacial (see light blue regions on Fig. 3e and across Queen Maud Land between ~20 W and 10 W on Fig. 7e) also produces a significant response in the predicted elevation driven δD trend. Across this region, there is a significant reduction, up to maximum of 20‰/kyr, from +20‰/kyr in REF_L to 0–(−)0.25‰/kyr in the REF_THIN model. It is noted that the magnitude of this response is significantly larger than that generated across this area when investigating the δD signal at the same core sites due to a WAIS collapse (~4‰/kyr, see Fig. 6 in Bradley et al., 2012).

4.2. Results for the REF_WB ice model

In contrast to the insensitivity of elevation changes at the East Antarctic ice core sites due to changes in the WAIS (Bradley et al., 2012), introducing a retreat of marine-based ice within the W–A basins in the REF_WB model produces a significant and notably larger

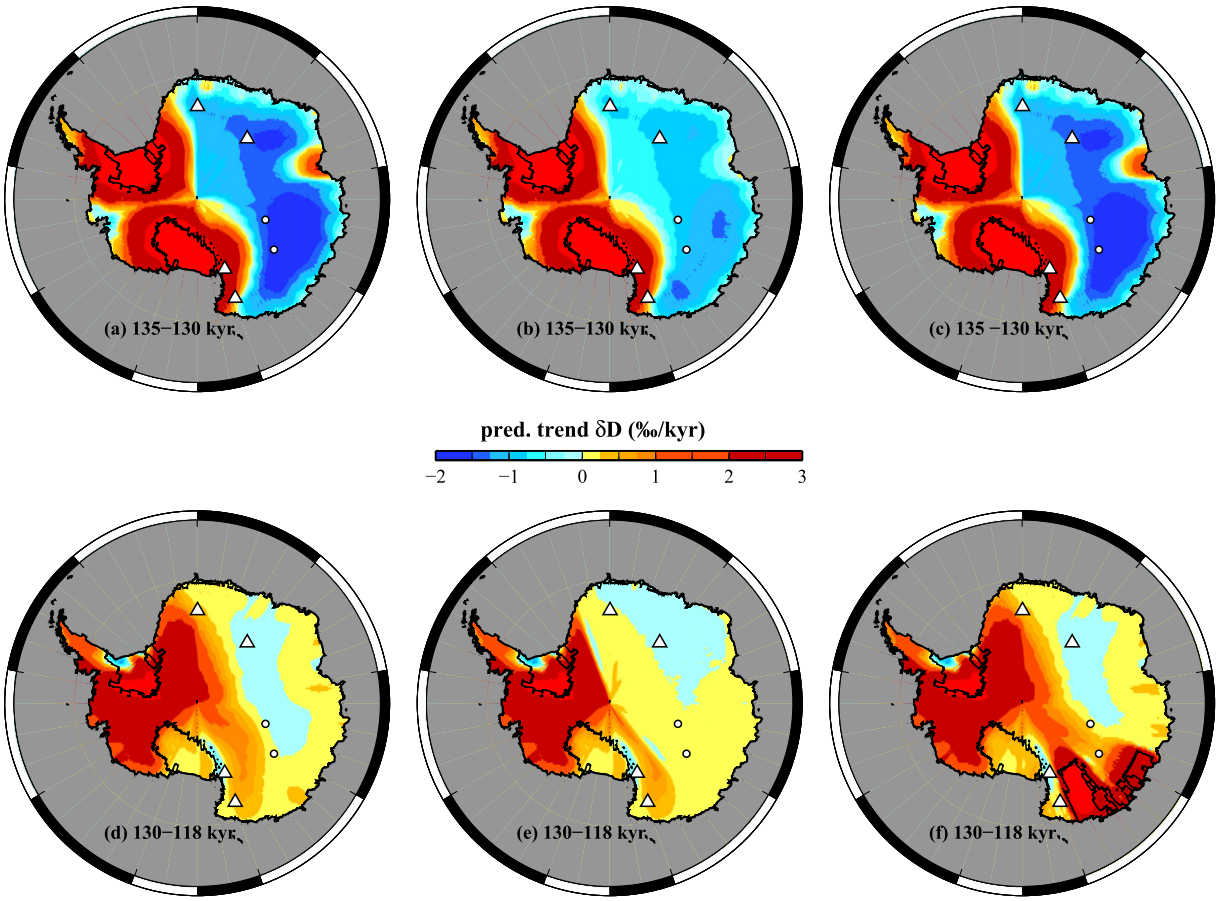

Fig. 7. Spatial plots of the elevation-driven predicted δD trend (‰/kyr) calculated for the three ice models discussed in the paper over two time intervals; between 135 and 130 kyr BP for (a) REF_L, (b) REF_THIN and (c) REF_WB and between 130 and 118 kyr BP for (d) REF_L, (e) REF_THIN and (f) REF_WB. On all plots the location of the 6 ice core sites is marked (see Table 1 with the black contour marking the edge of each ice model used). Note that the colour scale extends beyond the maximum/minimum values shown on the scale bar to −4.5/20‰/kyr for dark blue/dark red respectively.

and more widespread signal. Not surprisingly, the spatial response in the predicted elevation-driven δD (‰) signal has the greatest amplitude near the W–A basins. The magnitude of this signal (see Fig. 6) is greatest at TALDICE and EDC, with an increase relative to the REF_L results of up to (+) 18‰ and (−) 8‰ respectively. There is also a resolvable but significantly smaller signal at VK and TD of amplitude ~±1.5‰.

It is noted, however, that the change in the predicted δD signal at these two ice core sites now produces a significant misfit to the observed ice core data. For example, at TALDICE the magnitude of the δD peak is significantly over predicted compared to the maximum in the observed δD record (see Fig. 2) by at least 10‰. Also, the minor rise of 4‰ from 126 to 118 kyr BP within the REF_L model is largely removed, to only 1‰ using the REF_WB model. This rise was produced by adding a thinning of the ice sheet across the region to capture the observed trend in the ice core data (see Fig. 2) over this period. Secondly, a significant warming trend is now predicted at EDC (as seen by the +4‰ rise on Fig. 6) which is again not evident in the observed data (fall of 4‰). These results imply that the size and spatial extent of the simulated retreat is too large to be reconciled with the ice core data. However, the fact that these two ice core records are sensitive to such a retreat (as opposed to our results for a WAIS collapse; Bradley et al., 2012) there is potential to use these data to constrain a possible retreat of ice in this region. This is an important result given the distinct lack of other direct observational evidence to constrain such a retreat (see Jordan et al., 2010; Young et al., 2011; Wright et al., 2012).

The contribution to the total surface elevation change and predicted elevation-driven δD (‰) from movement of the SLS is more pronounced for REF_WB than for REF_THIN (Fig. 8).

Following the onset of the retreat at 130 kyr BP to the later part of the LIG, the magnitude of SLS change increases by up to 80 m compared to those in the REF_L results at sites located closets to W–A basins. At TALDICE an enhanced uplift (which would generate a cooling signal in the predicted δD) is produced relative to the REF_L results, whereas an enhanced subsidence (which would generate a warming signal in the predicted δD) is produced at EDC. An interesting aspect of these results, which differs from those above and in Bradley et al. (2012), is that the isostatic response (motion of the SLS) which now dominates the final predicted surface elevation driven response over the later part of the LIG at these two ice core sites, as opposed to the ice thickness changes. This is evident in Fig. 6 on comparing the black (REF_L) and green (REF_WB) lines: the local ice thickness changes are the same in the REF_L and REF_WB models and so the difference between these two curves at each site is due to the isostatic motion associated with ice retreat in the adjacent W-A basins.

In Fig. 7c and f, the inter-site variability is evident in the temporal nature and relative magnitude of the predicted elevation-driven δD trend in and around the W–A basins.

Over the first 5 kyr of the LIG, prior to the onset of the ice retreat across these basins (see Fig. 7c), there is a predicted fall in the elevation driven response of ~−4.5‰/kyr following the simulated retreat (see Fig. 7f) and significant thinning (fall in surface elevation) within

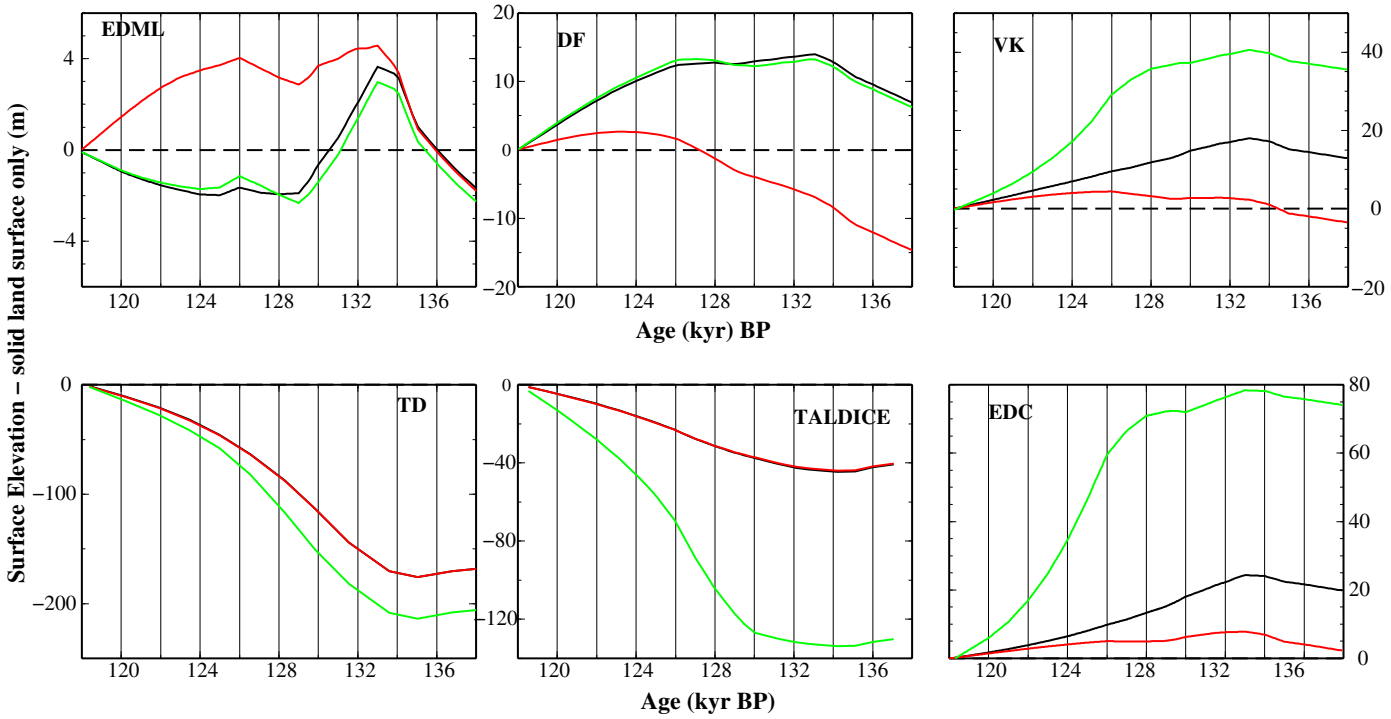

Fig. 8. The predicted relative surface elevation at each ice core sites due to movement of the solid land surface (SLS) only for the three ice models described: REF_L (solid black line); REF_THIN (solid red) and REF_WB (solid green). Note that results are shown for only for the intermediate earth model. As there were minimal changes between the REF_L and REF_THIN ice model at TALDICE and TD sites, the results for these two models (solid black and solid red line respectively) plot on top of each other. Note that the results tend towards zero as they have not been corrected to a present day value using the Bassett et al., 2007 model.

the basins, producing a significant increase in the predicted stable isotope rate (~20‰/kyr). In contrast, at sites surrounding the basin (such as EDC) where there is no change in the EAIS within the REF_WB model compared to the REF_L model, there is a fall of 0.25‰/kyr. Note that the magnitude of this response is larger than the predicted elevation driven trend results from a complete collapse of the WAIS, as shown on Fig. 6 in Bradley et al., 2012.

As discussed above, the predicted δD signal produced by the simulated retreat within the W-A basins as represented in the REF_WB ice model is not consistent with that observed in the ice core data. However, the results shown in Fig. 7(c and f), Figs. 6 and 8 at TALDICE and EDC, indicate how revisions to this retreat scenario and the expected response in the motion of the SLS (isostatic response), could be made such that the predicted signal would be more compatible with the observed data. For example, at TALDICE, the observed δD rise of 4‰ over the later part of the LIG was generated using the REF_L model by adding a thinning in the ice sheet, which is now overprinted due to the enhanced uplift within the REF_WB model. This implies that if an extensive spatial retreat did occur, the localised thinning of the ice sheet would need to be significantly increased to compensate. Alternatively, if a more restricted retreat was simulated with the Wilkes Basin, it is expected (given the results seen for EDC) via an enhanced subsidence across the region, a warming trend (rise) would be generated in the predicted δD, removing the requirement for localised thinning in the ice sheet.

These results show how there is clearly scope for using the difference in the late LIG δD between these two sites to assess the possibility of a significant and spatial extent of a retreat within these basins. Depending on the size of the retreat and associated isostatic response implications could be made about localised changes in the ice sheet. However, more accurate ice models that incorporate the appropriate physics should be applied in such an analysis. Furthermore, the contribution from climate effects on this spatial difference should also be considered to ensure a robust interpretation of the data-model comparison.

5. Conclusion

This study has examined the influence of ice surface elevation — due to ice thickness changes and the associated vertical motion of the solid land surface (SLS) on δD (‰) at six AIS ice core sites. Three LIG AIS models were used to examine the sensitivity of the elevation-driven δD signal to plausible variations in EAIS evolution during the LIG.

One primary aim of this study was to determine if the high δD value (or LIG overshoot) recorded in the ice core observations during this period (relative to the PIG) might include a significant elevation signal. It was found that adding a relatively moderate reduction in the amount of thickening across the central regions of the EAIS over the interglacial period introduces a significant (up to 8‰) elevation-driven δD signal at the central EAIS ice core sites (DF, EDC, VK and EDML) (see Fig. 6). This result shows that relatively small elevation changes may explain at least part of the LIG δD signal (as discussed by Holden et al., 2010). The potential contribution of this process must therefore be considered when using these records to estimate LIG temperatures and interactions between ice sheet topography and Antarctic regional climatic changes (temperature and accumulation).

A second main aim of this study was to examine if the ice core data are sensitive to ice retreat in a large sector of the EAIS that is marine-based — the Wilkes and Aurora basins. This aspect of our study is motivated by the current attribution problem for LIG sea levels and the lack of Antarctic near-field data to constrain plausible contributions from the AIS. Introducing a significant retreat of marine-based ice with the Wilkes and Aurora subglacial basins led to a distinct δD signal at the EAIS ice core sites proximal to the basins

(TD, TALDICE and EDC). Our results indicate that the differential signal between TALDICE and EDC could provide observational control on the geometry and amplitude of marine retreat in this region. However, more realistic ice models and the consideration of a possible climate signal will be required to ensure a robust interpretation of the observed signal.

Acknowledgements

This is a contribution to the PALSEA working group. This is Past4Future contribution no.24. The research leading to these results has received funding from the European Union's Seventh Framework Programme (FP7/2007-2013) under grant agreement no. 243908, "Past4Future. Climate change — learning from the past climate".

Mark Siddall is supported by an RCUK fellowship and the University of Bristol.

Glenn Milne acknowledges support from the Natural Sciences and Engineering Research Council of Canada and the Canada Research Chairs program.

Eric Wolff is supported by the British Antarctic Survey's Polar Science for Planet Earth programme, funded by NERC.

Valerie Masson-Delmotte acknowledges support by the ANR DOME A project (ANR-07-BLAN-0125).

The Talos Dome Ice core Project (TALDICE), a joint European programme, is funded by national contributions from Italy, France, Germany, Switzerland and the United Kingdom. Primary logistical support was provided by PNRA at Talos Dome. This is TALDICE publication no is 27.

Appendix A. Supplementary data

Supplementary data to this article can be found online at http://dx.doi.org/10.1016/j.gloplacha.2012.11.002.

References

Bamber, J.L., Riva, R.E.M., Vermeersen, B.L.A., LeBrocq, A.M., 2009. Reassessment of the potential sea-level rise from a collapse of the West Antarctic Ice Sheet. Science 324 (5929), 901–903.

Bassett, S.E., Milne, G.A., Mitrovica, J.X., Clark, P.U., 2005. Ice sheet and solid earth influences on far-field sea-level histories. Science 309 (5736), 925–928.

Bassett, S.E., Milne, G.A., Bentley, M.J., Huybrechts, P., 2007. Modelling Antarctic sea-level data to explore the possibility of a dominant Antarctic contribution to meltwater pulse IA. Quaternary Science Reviews 26 (17–18), 2113–2127.

Born, A., Nisancioglu, K.H., 2012. Melting of Northern Greenland during the last interglaciation. The Cryosphere 6, 1239–1250 http://dx.doi.org/10.5194/tc-6-1239-2012.

Bradley, S.L., Siddall, M., Milne, G.A., Masson-Delmotte, V., Wolff, E., 2012. Where might we find evidence of a Last Interglacial West Antarctic Ice Sheet collapse in Antarctic ice core records? Global and Planetary Change 88–89, 64–75.

Cuffey, K.M., Marshall, S.J., 2000. Substantial contribution to sea-level rise during the last interglacial from the Greenland ice sheet. Nature 404 (6778), 591–594.

Davis, J.L., Mitrovica, J.X., Scherneck, H.G., Fan, R., 1999. Investigations of Fennoscandian glacial isostatic adjustment using modern sea level records. Journal of Geophysical Research - Solid Earth 104 (B2), 2733–2747.

Denton, G.H., 2011. Palaeoclimate: East Antarctic retreat. Nature Geoscience 4 (3), 135–136.

Dutton, A., Lambeck, K., 2012. Ice volume and sea level during the Last Interglacial. Science 337 (6091), 216–219.

Dziewonski, A.M., Anderson, D.L., 1981. Preliminary reference earth model. Physics of the Earth and Planetary Interiors 25 (4), 297–356.

EPICA Members, 2006. One-to-one coupling of glacial climate variability in Greenland and Antarctica. Nature 444 (7116), 195–198.

Farrell, W.E., Clark, J.A., 1976. Postglacial sea-level. Geophysical Journal of the Royal Astronomical Society 46 (3), 647–667.

Forte, A.M., Mitrovica, J.X., 1996. New inferences of mantle viscosity from joint inversion of long-wavelength mantle convection and post-glacial rebound data. Geophysical Research Letters 23 (10), 1147–1150.

Gomez, N., Mitrovica, J.X., Tamisiea, M.E., Clark, P.U., 2010. A new projection of sea level change in response to collapse of marine sectors of the Antarctic Ice Sheet. Geophysical Journal International 180 (2), 623–634.

Grootes, P.M., Steig, E.J., Stuiver, M., Waddington, E.D., Morse, D.L., 2001. The Taylor dome antarctic O-18 record and globally synchronous changes in climate. Quaternary Research 56 (3), 289–298.

Haywood, A., Valdes, P.J., Sellwood, B.W., Kaplan, J.O., 2002. Antarctic climate during the middle Pliocene: model sensitivity to ice sheet variation. Palaeogeography, Palaeoclimatology, Palaeoecology 182 (1–2), 93–115.

Helsen, M.M., van de Wal, R.S.W., van den Broeke, M.R., van de Berg, W.J., Oerlemans, J., 2012. Coupling of climate models and ice sheet models by surface mass balance gradients: application to the Greenland Ice Sheet. The Cryosphere 6 (2).

Helsen, M.M., van de Wal, R.S.W., van den Broeke, M.R., van de Berg, W.J. and Oerlemans, J., submitted for publication. Limited Greenland ice loss during the Eemian. Nature.

Hill, D.J., Haywood, A.M., Hindmarsh, R.C.A., Valdes, P.J., 2007. Characterizing ice sheets during the Pliocene: evidence from data and models. Deep-Time Perspectives on Climate Change: Marrying the Signal from Computer Models and Biological Proxies. Geological Soc Publishing House, Bath (517–538 pp.).

Holden, P.B., Edwards, N.R., Wolff, E.W., Lang, N.J., Singarayer, J.S., Valdes, P.J., Stocker, T.F., 2010. Interhemispheric coupling, the West Antarctic Ice Sheet and warm Antarctic interglacials. Climate of the Past 6 (4), 431–443.

Huang, F.X., Liu, X.H., Kong, P., Fink, D., Ju, Y.T., Fang, A.M., Yu, L.J., Li, X.L., Na, C.G., 2008. Fluctuation history of the interior East Antarctic Ice Sheet since mid-Pliocene. Antarctic Science 20 (2), 197–203.

Huybrechts, P., 2002. Sea-level changes at the LGM from ice-dynamic reconstructions of the Greenland and Antarctic ice sheets during the glacial cycles. Quaternary Science Reviews 21 (1–3), 203–231.

Huybrechts, P., Goelzer, H., Janssens, I., Driesschaert, E., Fichefet, T., Goosse, H., Loutre, M.F., 2011. Response of the Greenland and Antarctic Ice Sheets to multi-millennial greenhouse warming in the Earth System Model of Intermediate Complexity LOVECLIM. Surveys in Geophysics 32 (4–5), 397–416.

Jordan, T.A., Ferraccioli, F., Corr, H., Graham, A., Armadillo, E., Bozzo, E., 2010. Hypothesis for mega-outburst flooding from a Palaeo-subglacial lake beneath the East Antarctic Ice Sheet. Terra Nova 22 (4), 283–289.

Jouzel, J., Barkov, N.I., Barnola, J.M., Bender, M., Chappellaz, J., Genthon, C., Kotlyakov, V.M., Lipenkov, V., Lorius, C., Petit, J.R., Raynaud, D., Raisbeck, G., Ritz, C., Sowers, T., Stievenard, M., Yiou, F., Yiou, P., 1993. Extending the Vostok Ice-Core Record of the Paleoclimate to the Penultimate Glacial Period. Nature 364 (6436), 407–412.

Jouzel, J., Masson-Delmotte, V., Cattani, O., Dreyfus, G., Falourd, S., Hoffmann, G., Minster, B., Nouet, J., Barnola, J.M., Chappellaz, J., Fischer, H., Gallet, J.C., Johnsen, S., Leuenberger, M., Loulergue, L., Luethi, D., Oerter, H., Parrenin, F., Raisbeck, G., Raynaud, D., Schilt, A., Schwander, J., Selmo, E., Souchez, R., Spahni, R., Stauffer, B., Steffensen, J.P., Stenni, B., Stocker, T.F., Tison, J.L., Werner, M., Wolff, E.W., 2007. Orbital and millennial Antarctic climate variability over the past 800,000 years. Science 317 (5839), 793–796.

Kaufmann, G., Lambeck, K., 2002. Glacial isostatic adjustment and the radial viscosity profile from inverse modeling. Journal of Geophysical Research - Solid Earth 107 (B11), 15.

Kendall, R.A., Mitrovica, J.X., Milne, G.A., 2005. On post-glacial sea level — II. Numerical formulation and comparative results on spherically symmetric models. Geophysical Journal International 161 (3), 679–706.

Kopp, R.E., Simons, F.J., Mitrovica, J.X., Maloof, A.C., Oppenheimer, M., 2009. Probabilistic assessment of sea level during the last interglacial stage. Nature 462 (7275), 863–867.

Laepple, T., Werner, M., Lohmann, G., 2011. Synchronicity of Antarctic temperatures and local solar insolation on orbital timescales. Nature 471 (7336), 91–94.

Lambeck, K., Purcell, A., Dutton, A., 2012. The anatomy of interglacial sea levels: The relationship between sea levels and ice volumes during the Last Interglacial. Earth and Planetary Science Letters 315–316 (0), 4–11.

Lang, N., Wolff, E.W., 2011. Interglacial and glacial variability from the last 800 ka in marine, ice and terrestrial archives. Climate of the Past 7 (2), 361–380.

Le Brocq, A.M., Payne, A.J., Vieli, A., 2010. An improved Antarctic dataset for high resolution numerical ice sheet models (ALBMAP v1). Earth System Science Data Discussions 3 (1), 195–230.

Lilly, K., Fink, D., Fabel, D., Lambeck, K., 2010. Pleistocene dynamics of the interior East Antarctic ice sheet. Geology 38 (8), 703–706.

Liu, X., Huang, F., Kong, P., Fang, A., Li, X., Ju, Y., 2010. History of ice sheet elevation in East Antarctica: Paleoclimatic implications. Earth and Planetary Science Letters 290 (3–4), 281–288.

Mackintosh, A., Golledge, N., Domack, E., Dunbar, R., Leventer, A., White, D., Pollard, D., DeConto, R., Fink, D., Zwartz, D., Gore, D., Lavoie, C., 2011. Retreat of the East Antarctic ice sheet during the last glacial termination. Nature Geosci 4 (3), 195–202.

Masson-Delmotte, V., Hou, S., Ekaykin, A., Jouzel, J., Aristarain, A., Bernardo, R.T., Bromwich, D., Cattani, O., Delmotte, M., Falourd, S., Frezzotti, M., Gallee, H., Genoni, L., Isaksson, E., Landais, A., Helsen, M.M., Hoffmann, G., Lopez, J., Morgan, V., Motoyama, H., Noone, D., Oerter, H., Petit, J.R., Royer, A., Uemura, R., Schmidt, G.A., Schlosser, E., Simoes, J.C., Steig, E.J., Stenni, B., Stievenard, M., van den Broeke, M.R., de Wal, R., de Berg, W.J.V., Vimeux, F., White, J.W.C., 2008. A review of Antarctic surface snow isotopic composition: observations, atmospheric circulation, and isotopic modeling. Journal of Climate 21 (13), 3359–3387.

Masson-Delmotte, V., Stenni, B., Pol, K., Braconnot, P., Cattani, O., Falourd, S., Kageyama, M., Jouzel, J., Landais, A., Minster, B., Barnola, J.M., Chappellaz, J., Krinner, G., Johnsen, S., Röthlisberger, R., Hansen, J., Mikolajewicz, U., Otto-Bliesner, B., 2010. EPICA Dome C record of glacial and interglacial intensities. Quaternary Science Reviews 29 (1–2), 113–128.

Masson-Delmotte, V., Buiron, D., Ekaykin, A., Frezzotti, M., Gallee, H., Jouzel, J., Krinner, G., Landais, A., Motoyama, H., Oerter, H., Pol, K., Pollard, D., Ritz, C., Schlosser, E., Sime, L.C., Sodemann, H., Stenni, B., Uemura, R., Vimeux, F., 2011. A comparison of the present and last interglacial periods in six Antarctic ice cores. Climate of the Past 7 (2), 397–423.

McKay, N.P., Overpeck, J.T., Otto-Bliesner, B.L., 2011. The role of ocean thermal expansion in Last Interglacial sea level rise. Geophysical Research Letters 38, 6.
Mercer, J.H., 1978. West antarctic ice sheet and CO2 greenhouse effect - threat of disaster. Nature 271 (5643), 321–325.
Milne, G.A., Mitrovica, J.X., 1998. Postglacial sea-level change on a rotating Earth. Geophysical Journal International 133 (1), 1–19.
Mitrovica, J.X., Milne, G.A., 2003. On post-glacial sea level: I. General theory. Geophysical Journal International 154 (2), 253–267.
Mitrovica, J.X., Davis, J.L., Shapiro, I.I., 1994. A spectral formalism for computing 3-dimensional deformations due to surface loads.1. theory. Journal of Geophysical Research - Solid Earth 99 (B4), 7057–7073.
Mitrovica, J.X., Milne, G.A., Davis, J.L., 2001. Glacial isostatic adjustment on a rotating earth. Geophysical Journal International 147 (3), 562–578.
Mitrovica, J.X., Wahr, J., Matsuyama, I., Paulson, A., 2005. The rotational stability of an ice-age earth. Geophysical Journal International 161 (2), 491–506.
Morelli, A., Danesi, S., 2004. Seismological imaging of the Antarctic continental lithosphere: a review. Global and Planetary Change 42 (1–4), 155–165.
NEEM community members, in revision. Eemian interglacial reconstructed from a Greenland folded ice core. Nature.
Otto-Bliesner, B.L., Marsha, S.J., Overpeck, J.T., Miller, G.H., Hu, A.X., 2006. Simulating arctic climate warmth and icefield retreat in the last interglaciation. Science 311 (5768), 1751–1753.
Parrenin, F., Barnola, J.M., Beer, J., Blunier, T., Castellano, E., Chappellaz, J., Dreyfus, G., Fischer, H., Fujita, S., Jouzel, J., Kawamura, K., Lemieux-Dudon, B., Loulergue, L., Masson-Delmotte, V., Narcisi, B., Petit, J.R., Raisbeck, G., Raynaud, D., Ruth, U., Schwander, J., Severi, M., Spahni, R., Steffensen, J.P., Svensson, A., Udisti, R., Waelbroeck, C., Wolff, E., 2007. The EDC3 chronology for the EPICA dome C ice core. Climate of the Past 3 (3), 485–497.
Pierce, E.L., Williams, T., van de Flierdt, T., Hemming, S.R., Goldstein, S.L., Brachfeld, S.A., 2011. Characterizing the sediment provenance of East Antarctica's weak underbelly: the Aurora and Wilkes sub-glacial basins. Paleoceanography 26.
Pingree, K., Lurie, M., Hughes, T., 2011. Is the East Antarctic ice sheet stable? Quaternary Research 75 (3), 417–429.
Quiquet, A., Punge, H.J., Ritz, C., Fettweis, X., Kageyama, M., Krinner, G., Salas, D., Sjolte, J., 2012. Large sensitivity of a Greenland ice sheet model to atmospheric forcing fields. The Cryosphere Discussions 6 (2).
Radi, Valentina, Hock, R., 2010. Regional and global volumes of glaciers derived from statistical upscaling of glacier inventory data. Journal of Geophysical Research 115 (F1), F01010.
Robinson, A., Calov, R., Ganopolski, A., 2011. Greenland ice sheet model parameters constrained using simulations of the Eemian Interglacial. Climate of the Past 7 (2), 381–396.
Siddall, M., Milne, G.A., Masson-Delmotte, V., 2012. Uncertainties in elevation changes and their impact on Antarctic temperature records since the end of the last glacial period. Earth and Planetary Science Letters 315–316, 12–23.
Siegert, M.J., Taylor, J., Payne, A.J., 2005. Spectral roughness of subglacial topography and implications for former ice-sheet dynamics in East Antarctica. Global and Planetary Change 45 (1–3), 249–263.
Sime, L.C., Wolff, E.W., Oliver, K.I.C., Tindall, J.C., 2009. Evidence for warmer interglacials in East Antarctic ice cores. Nature 462 (7271), 342–345.
Stenni, B., Masson-Delmotte, V., Selmo, E., Oerter, H., Meyer, H., Röthlisberger, R., Jouzel, J., Cattani, O., Falourd, S., Fischer, H., Hoffmann, G., Iacumin, P., Johnsen, S.J., Minster, B., Udisti, R., 2010. The deuterium excess records of EPICA Dome C and Dronning Maud Land ice cores (East Antarctica). Quaternary Science Reviews 29 (1–2), 146–159.
Stone, E.J., Lunt, D.J., Annan, J.D., Hargreaves, J.C., 2012. Quantification of the Greenland ice sheet contribution to Last Interglacial sea-level rise. Climate of the Past Discussions 8 (4).
Uemura, R., Masson-Delmotte, V., Jouzel, J., Landais, A., Motoyama, H., Stenni, B., 2012. Ranges of moisture-source temperature estimated from Antarctic ice cores stable isotope records over glacialâ€“interglacial cycles. Climate of the Past 8 (3).
Vaughan, D.G., Spouge, J.R., 2002. Risk Estimation of Collapse of the West Antarctic Ice Sheet. Climatic Change 52 (1), 65–91.
Vinther, B.M., Buchardt, S.L., Clausen, H.B., Dahl-Jensen, D., Johnsen, S.J., Fisher, D.A., Koerner, R.M., Raynaud, D., Lipenkov, V., Andersen, K.K., Blunier, T., Rasmussen, S.O., Steffensen, J.P., Svensson, A.M., 2009. Holocene thinning of the Greenland ice sheet. Nature 461 (7262), 385–388.
Watanabe, O., Jouzel, J., Johnsen, S., Parrenin, F., Shoji, H., Yoshida, N., 2003. Homogeneous climate variability across East Antarctica over the past three glacial cycles. Nature 422 (6931), 509–512.
Weertman, J., 1976. Glaciologys grand unsolved problem. Nature 260 (5549), 284–286.
Whitehouse, P.L., Bentley, M.J., Le Brocq, A.M., 2012. A deglacial model for Antarctica: geological constraints and glaciological modelling as a basis for a new model of Antarctic glacial isostatic adjustment. Quaternary Science Reviews 32, 1–24.
Wright, A.P., Young, D.A., Roberts, J.L., Schroeder, D.M., Bamber, J.L., Dowdeswell, J.A., Young, N.W., Le Brocq, A.M., Warner, R.C., Payne, A.J., Blankenship, D.D., van Ommen, T.D., Siegert, M.J., 2012. Evidence of a hydrological connection between the ice divide and ice sheet margin in the Aurora Subglacial Basin, East Antarctica. Journal of Geophysical Research - Earth Surface 117.
Young, D.A., Wright, A.P., Roberts, J.L., Warner, R.C., Young, N.W., Greenbaum, J.S., Schroeder, D.M., Holt, J.W., Sugden, D.E., Blankenship, D.D., van Ommen, T.D., Siegert, M.J., 2011. A dynamic early East Antarctic Ice Sheet suggested by ice-covered fjord landscapes. Nature 474 (7349), 72–75.